



NOVA

University of Newcastle Research Online

nova.newcastle.edu.au

Hyder, Md Mashud; Khan, Reduan H.; Mahata, Kaushik; Khan, Jamil Y. "A predictive protection scheme based on adaptive synchrophasor communications". Published in Proceedings of the IEEE International Conference on Smart Grid Communications (Vancouver, Canada 21-24 October, 2013) p. 762-767 (2013)

Available from: <http://dx.doi.org/10.1109/SmartGridComm.2013.6688051>

© 2013 IEEE. Personal use of this material is permitted. Permission from IEEE must be obtained for all other uses, in any current or future media, including reprinting /republishing this material for advertising or promotional purposes, creating new collective works, for resale or redistribution to servers or lists, or reuse of any copyrighted component of this work in other works.

Accessed from: <http://hdl.handle.net/1959.13/1317641>

A Predictive Protection Scheme based on Adaptive Synchrophasor Communications

Md Mashud Hyder, Reduan H. Khan, Kaushik Mahata, Jamil Y. Khan
School of Electrical Engineering and Computer Science
The University of Newcastle, NSW 2308, Australia

Abstract—This paper presents a conceptual design of a synchrophasor based protection and control scheme that uses an efficient communications scheme to timely predict the voltage instability point of a local bus. A voltage instability prediction algorithm is proposed that fits a set of algebraic equations to the measured synchrophasor data and performs some efficient computations to predict when the load profile of the local bus will reach the critical point. To keep the communications load of the scheme minimum, the novel concept of adaptive synchrophasor reporting is introduced that dynamically switches between a normal and an expedited reporting rate based on the output of the prediction algorithm. The performance of the proposed protection scheme is demonstrated by using the New England 39-bus system. Also, the performance of the communications scheme is analyzed through an OPNET simulation model using an IEEE 802.16/WiMAX based wireless communications network.

I. INTRODUCTION

Timely identification of voltage instability is one of the major concerns in power system planning and operation. By making use of real time synchrophasor measurements from the Phasor measurement units (PMUs), the power control system can determine the characteristics of a voltage instability event and predict an out-of-step condition using a time-series expansion algorithm. When the voltage of a load-bus reaches close to its instability point, an aggressive synchrophasor reporting rate may enhance the performance of the time-series algorithm to better predict the transient response of the system and allow the control system to execute appropriate actions within the incubation period [1].

However, an aggressive reporting rate comes at a cost of higher bandwidth requirement. This is particularly challenging to a wireless based multi-service smart grid communications network where the locked radio resources may cause bandwidth-starvation to the other applications. This problem can be solved using an adaptive reporting scheme where the controller dynamically switches between a normal and an expedited reporting rate based on the output of the prediction algorithm. Such a scheme is reasonable since a voltage instability event in a power system is a highly random phenomenon. For most of the time, the system will operate normally and the synchrophasor reporting rates can be maintained at an optimum level based on the application requirements.

PMU based voltage instability monitoring can be classified into two broad categories: i) methods requiring the global phasor measurements [2]; ii) methods using only local phasor data [3], [4]. A major challenge for the global methods is to aggregate the synchrophasor measurements from the

whole system. Moreover, they need to construct the system Jacobian for tracking the dynamics of the system which is computationally expensive. In contrast, a local method needs information from only the local buses and hence effective for implementing online protection schemes. The proposed work belongs to the second category.

A number of methods has been proposed for detecting a local voltage instability event. Two-bus Thevenin equivalent model of power system has been used for voltage instability detection in [2], [5]. The method proposed in [2] is based on a comparison of the Thevenin equivalent impedance as seen from the load bus and the apparent impedance of the load. The main difficulty in such an approach is to estimate the time-varying Thevenin equivalent parameters [5]. Furthermore, the Thevenin equivalent does not include the detailed dynamics of the system and therefore, does not reflect a continuous change in the system states. The voltage magnitudes of local buses are also used for voltage stability monitoring [6], [3]. A voltage stability risk index is used in [6] to identify the vulnerability of the system in terms of voltage instability. The work in [3] monitors the magnitude of voltages along with the voltage decline rates of all buses. However, selection of an appropriate threshold for voltage stability index is a critical task.

In this paper, we propose a novel prediction algorithm for voltage instability detection based on the local synchrophasor measurements. Two key challenges for such algorithms are the complex power system dynamics and the presence of voltage-sensitive loads i.e. ZIP loads that make the prediction task more complicated [7], [5]. To alleviate these difficulties, we first develop a set of equations that can approximately express the power consumption profile of different buses in terms of bus voltage phasor. We then periodically estimate the maximum loadability and voltage instability point of the system by utilizing the local synchrophasor measurements and a curve-fitting technique. The curve fitting technique leads to an optimization problem which we solve efficiently using a convex programming.

Moreover, we propose an adaptive synchrophasor reporting scheme that dynamically switches between a normal and an expedited reporting rate based on the output of the prediction algorithm in order to keep the communications load minimum. Note that the proposed protection scheme is agnostic to the underlying communications media as long as its bandwidth and latency requirements are met. Nonetheless, we have used an IEEE802.16 based WiMAX communication system as a proof of concept for this study. The performance of the proposed

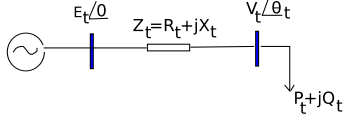


Fig. 1. Two-bus Thevenin equivalent system. Load bus and the rest of the system is represented by a voltage source (E) and transmission line.

protection scheme is demonstrated by using the New England 39-bus system. Also, the performance of the communications scheme is analyzed through an OPNET simulation model. The results indicate that the proposed voltage instability prediction algorithm along with the adaptive synchrophasor reporting scheme allows the control system to take timely action and reduces the possibility of false alarm at the expense of minimum communications load.

II. PROBLEM STATEMENT

Let us consider a power system network where a local bus consuming power $P_t + jQ_t$ at time t . The local voltage stability monitoring techniques [2] generally convert the whole power system network into a time dependent two-bus Thevenin equivalent system (Figure 1) where a generator $E_t \angle 0$ supplies power $P_t + jQ_t$ to the local bus through a transmission line $Z_t = R_t + jX_t$. The voltage phasor of local bus be $V_t \angle \theta_t$. The real and reactive power transfer to the local bus can be expressed as [4]

$$P_t = \frac{V_t}{|Z_t|^2} [(E_t \cos \theta_t - V_t)R_t - E_t \sin \theta_t X_t] \quad (1)$$

$$Q_t = \frac{V_t}{|Z_t|^2} [(E_t \cos \theta_t - V_t)X_t + E_t \sin \theta_t R_t] \quad (2)$$

Both P_t and Q_t are functions of five variables i.e., E_t, V_t, θ_t, X_t and R_t . Different assumptions have been used to estimate the future profiles of P_t and Q_t [4], [2]. A compact expression of maximum active and reactive power transfer limit to a local bus has been developed in [4] by assuming R_t/X_t is small and E_t, X_t and Q_t or P_t are constant: $P_{\max} = \sqrt{\frac{E_t^4}{4X_t^2} - Q_t \frac{E_t^2}{X_t}}$; $Q_{\max} = \frac{E_t^2}{4X_t} - P_t^2 \frac{X_t}{E_t^2}$. However, the method cannot perform well when the load in a local bus is voltage-sensitive. The case of voltage-sensitive load i.e., ZIP load is considered in [2]. The ZIP load is modeled as [7], [2]

$$P_t = k_t(P_c + a_1 V_t + a_2 V_t^2) \quad (3)$$

$$Q_t = k_t(Q_c + b_1 V_t + b_2 V_t^2) \quad (4)$$

where $P_c, Q_c, a_1, a_2, b_1, b_2$ are constants and the value of k_t is an independent demand variable called *loading factor* [2]. The loading factor k_t can be used as an indication of the customer load demand changing with time. By combining (1) and (2) a relationship is developed in [2]

$$V_t^4 + V_t^2[2(P_t R_t + Q_t X_t) - E_t^2] + Z_t^2(P_t^2 + Q_t^2) = 0 \quad (5)$$

Let us draw the P-V characteristics curve from (5) by assuming Q_t, E_t, X_t are constant (Figure 2). We can also draw a set of ZIP load characteristics curves i.e. (P_t - V_t) curves by using (3) for different values of k_t . The system remains voltage stable

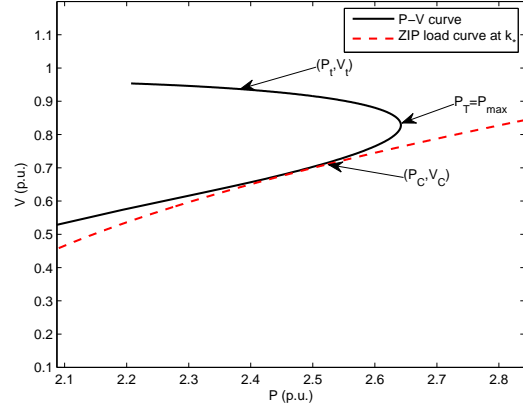


Fig. 2. PV curve of a typical load bus and ZIP load curve at critical k_* .

for a loading factor k_t if the ZIP load characteristics curve (3) for the k_t intersects the P-V curve at least two points [2]. The system becomes voltage unstable, when for some critical loading factor k_* , the ZIP curve becomes tangent to the system P-V curve.

In Figure 2, the system become voltage unstable when the voltage and the active power supply of the local bus become V_C and P_C p.u. respectively. We can make some interesting observations from the Figure 2. When the load demand increases, the power transfer increases and the voltage decreases until it reaches the maximum power transfer P_{\max} limit of the local bus. However, the voltage instability occurs at V_C, P_C which is beyond the maximum power transfer point P_{\max} .

Let the voltage and current phasor of a load bus are sampled using PMU at the discrete sampling instants $\{t_r\}_{r=1,2,\dots}$. The system can transfer maximum power P_{\max} to the bus at time T . The load bus voltage corresponding to P_{\max} be V_{pm} . If the load demand increases continuously, the system become voltage unstable at time C with power transfer and voltage being (P_C, V_C) . Let us consider a time instant t_ℓ . Let the prediction of P_{\max}, V_{pm} and V_C at t_ℓ are $P_{\max}^\ell, V_{pm}^\ell$ and V_C^ℓ respectively. We want to develop an efficient prediction algorithm such that

- $\|P_{\max} - P_{\max}^\ell\|, \|V_{pm} - V_{pm}^\ell\|$ and $\|V_C - V_C^\ell\|$ are small.
- $(T - t_\ell)$ and $(C - t_\ell)$ are large.

We assume that we have estimated the ZIP load parameters i.e., $P_c, Q_c, a_1, a_2, b_1, b_2$ in (3) (see [8]).

III. PREDICTION OF VOLTAGE INSTABILITY

By combining (1) and (2) we have

$$P_t = \frac{Q_t X_t}{R_t} + \frac{V_t E_t}{R_t} \cos \theta_t - \frac{V_t^2}{R_t} \quad (6)$$

By assuming Q_t, X_t, E_t, θ_t remain constant over a short time interval $t_{(\ell-n)}$ to t_ℓ (with $\ell > n$), we can write

$$P_t = \alpha_1(\ell) + \alpha_2(\ell)V_t + \alpha_3(\ell)V_t^2, \quad t \in [t_{\ell-n}, t_\ell] \quad (7)$$

where $\alpha_1(\ell) = \frac{Q_t X_t}{R_t}, \alpha_2(\ell) = \frac{E_t}{R_t} \cos \theta_t, \alpha_3(\ell) = -1/R_t$ remains constant in the fixed time interval. This assumption

is common in some state-of-art techniques [4], [2]. We can calculate the values of $\alpha_1(\ell), \alpha_2(\ell), \alpha_3(\ell)$ by using the past n time sampled data

$$\begin{bmatrix} 1 & V_{t_\ell} & V_{t_\ell}^2 \\ 1 & V_{t_{\ell-1}} & V_{t_{\ell-1}}^2 \\ \vdots & \vdots & \vdots \\ 1 & V_{t_{\ell-n+1}} & V_{t_{\ell-n+1}}^2 \end{bmatrix} \begin{bmatrix} \alpha_1(\ell) \\ \alpha_2(\ell) \\ \alpha_3(\ell) \end{bmatrix} = \begin{bmatrix} P_{t_\ell} \\ P_{t_{\ell-1}} \\ \vdots \\ P_{t_{\ell-n+1}} \end{bmatrix} \quad (8)$$

i.e. $A_v \alpha = \mathbf{y}$ (9)

and solving an optimization like

$$\min_{\alpha} \|\mathbf{y} - A_v \alpha\|_2 \quad (10)$$

where, $\mathbf{y} = [P_{t_\ell}, P_{t_{\ell-1}}, \dots, P_{t_{\ell-n+1}}]^T$, and \mathbf{x}^T indicates transpose of vector \mathbf{x} . The equation (7) will construct a parabola. If the parabola can follow the P-V characteristics curve (Figure 2), then the maximum load transfer P_{\max} can be approximated by using the focus of the parabola,

$$P_{\max}^\ell = \frac{\alpha_2(\ell)^2 + 4\alpha_3(\ell)\alpha_1(\ell)}{4\alpha_3(\ell)} \quad (11)$$

By combining (3) and (7), it can be shown that the ZIP load curve will intersect the parabola load curve at

$$V_i = \frac{-(\alpha_2(\ell) - k_t a_1) \pm \Gamma}{2(\alpha_3(\ell) - k_t a_2)} \quad (12)$$

where,

$$\Gamma = \sqrt{(\alpha_2(\ell) - k_t a_1)^2 - 4(\alpha_3(\ell) - k_t a_2)(\alpha_1(\ell) - k_t P_c)}$$

At critical loading k_* , the value of $\Gamma = 0$. Hence

$$k_* = \frac{-q \pm \sqrt{q^2 - 4(a_1^2 - 4P_c a_2)(\alpha_2(\ell)^2 - 4\alpha_1(\ell)\alpha_3(\ell))}}{2(a_1^2 - 4P_c a_2)} \quad (13)$$

where, $q = 4\alpha_3(\ell)P_c + 4\alpha_1(\ell)a_2 - 2\alpha_2(\ell)^2 a_1$.

The prediction P_{\max}^ℓ and k_* will be accurate if the values of Q_t, X_t, E_t, θ_t will remain constant throughout the time t_ℓ to $t = C$. However, it true only for small values of n . Furthermore, the voltage stabilizer of modern power system keeps the voltage profile virtually fixed [9], until it reaches closer to the instability point. Hence, it is difficult to predict the P-V characteristics of a system by using sampled data when $T - t_\ell$ is not small. Therefore, developing an prediction algorithm by only observing the P-V characteristics may not be reliable. To overcome the difficulty, we also estimate the P- θ characteristics of the system. Let us consider (1). By assuming E_t, X_t, V_t remain constant over a short interval $t_{(\ell-n)}$ to t_ℓ , we can write

$$P_t = \beta_1(\ell) + \beta_2(\ell) \cos \theta_t + \beta_3(\ell) \sin \theta_t, ; t \in [t_{\ell-n}, t_\ell] \quad (14)$$

By using the approaches (8),(10), we can estimate β and hence the P- θ characteristics curve. The maximum of the curve in (14) (say \hat{P}_{\max}^ℓ) will be an estimate of P_{\max} .

Let at time t_ℓ , the estimation error $\|P_{\max} - \hat{P}_{\max}^\ell\|$ is smaller than $\|P_{\max} - P_{\max}^\ell\|$, i.e., the P- θ curve approximate the P_{\max}

TABLE I
PREDICTION ALGORITHM

1. Calculate the parameters of (18) for all load buses.
2. If $\Delta V^s > \xi$ then
 3. Initialize the adaptive PMU reporting scheme (Section IV).
 4. Calculate the values of α and β in (7), (14) respectively, by using (10). Compute P_{\max}^ℓ and \hat{P}_{\max}^ℓ using (11) and (14).
 5. If $|P_{\max}^\ell - \hat{P}_{\max}^\ell| > \epsilon$, then
 6. Compare prediction accuracy of P_{\max} by P_{\max}^ℓ and \hat{P}_{\max}^ℓ using Section III-A.
 7. If the prediction accuracy by \hat{P}_{\max}^ℓ is higher, then
 8. Update the value of α in (7) by using the optimization in (15).
 9. End If
 10. End if
11. Compute the magnitude of voltage V_{pm}^ℓ corresponding to the maximum power transfer P_{\max}^ℓ by using (7). Estimate unstable voltage V_C^ℓ by using (12):
$$V_C^\ell = \frac{-(\alpha_2(\ell) - k_* a_1)}{2(\alpha_3(\ell) - k_* a_2)}$$
12. Approximate the times t_{pm}, t_s required to reach the voltage of bus s to V_{pm}^ℓ and V_C^ℓ respectively.
$$V_{t_\ell}^s - V_{pm}^\ell = \Delta V_{t_\ell}^s t_{pm} + \frac{1}{2} \delta (\Delta V_{t_\ell}^s) t_{pm}^2$$

$$V_{t_\ell}^s - V_C^\ell = \Delta V_{t_\ell}^s t_s + \frac{1}{2} \delta (\Delta V_{t_\ell}^s) t_s^2$$
13. If $V_{t_\ell}^s > V_{pm}^\ell$, then
 15. Set $t_*^s = t_s$ and $V_*^s = V_C^\ell$;
 14. Else t_*^s will be estimated using:
$$V_{t_\ell}^s - V_*^s = \Delta V_{t_\ell}^s t_*^s + \frac{1}{2} \delta (\Delta V_{t_\ell}^s) (t_*^s)^2$$

The value of t_*^s approximates the time required to move the voltage of bus s i.e. $V_{t_\ell}^s$ to the point of instability i.e. V_C .
 15. End If
18. If $t_* < \eta$ then
 19. Take proper control action to manage load on bus s to avoid possible voltage instability. The value of η will be determined by the latency of communication and control system.
 20. End If
21. End If

more accurately than P-V curve¹. However, we have to use P-V curve and (7), (12) to detect voltage instability point V_C . Hence we need to improve the prediction accuracy of the P-V curve by using (7). In this work, we do this by moving P_{\max}^ℓ closer to \hat{P}_{\max}^ℓ , i.e. we redefine the optimization (10)

$$\begin{aligned} & \min_{\alpha} \|\mathbf{y} - A_v \alpha\|_2 \quad (15) \\ & \text{sub. to } \frac{\alpha_2(\ell)^2 + 4\alpha_3(\ell)\alpha_1(\ell)}{4\alpha_3(\ell)} = \hat{P}_{\max}^\ell \end{aligned}$$

The optimization cannot be solved directly. Hence, we modify the optimization in the following way. If $P_{\max}^\ell > \hat{P}_{\max}^\ell$ then

$$\min_{\alpha} \|\mathbf{y} - A_v \alpha\|_2; \text{sub. to } \frac{\alpha_2(\ell)^2 + 4\alpha_3(\ell)\alpha_1(\ell)}{4\alpha_3(\ell)} \leq \hat{P}_{\max}^\ell. \quad (16)$$

However, if $P_{\max}^\ell < \hat{P}_{\max}^\ell$ then the optimization becomes difficult and we approximate the solution in the following way

$$\min_{\alpha, z} z + \tau \|\mathbf{y} - A_v \alpha\|_2 \quad (17)$$

$$\text{sub. to, } 4(\hat{P}_{\max}^\ell - \alpha_1(\ell)) = z; \quad \alpha_2(\ell)^2 - \alpha_3(\ell)z \leq 0$$

where $\tau > 0$ is a tuning factor (see Section III-C). Both (16) and (17) are convex and has only four variables.

¹A procedure of identifying prediction accuracy will be described in Section III-A.

A. Comparison of prediction accuracy of P_{\max} by different curves

Let the system will transfer P_{\max} at $t = T$ sec. If the system P-V curve follows the expression in (7) approximately, one may expect that the prediction accuracy of P_{\max} will increase when $|t_\ell - T|$ becomes smaller, where $|\cdot|$ indicates absolute value. Let the prediction of P_{\max} be P_{\max}^ℓ and prediction error $e_\ell = |P_{\max}^\ell - P_{\max}|$. Consider a time sequence $\{t_{\ell_i}\}_{i=1}^m$ such that $|t_{\ell_1} - T| > |t_{\ell_2} - T| \cdots > |t_{\ell_m} - T|$. Then we may expect $e_{\ell_1} > e_{\ell_2} > \cdots > e_{\ell_m}$. Let another different equation is also applied to estimate P_{\max} and its estimation error is indicated by $\hat{e}_{\ell_i} = |\hat{P}_{\max}^{\ell_i} - P_{\max}|$. Let $\hat{P}_{\max}^{\ell_i}$ is closer to P_{\max} than $P_{\max}^{\ell_i}$, i.e., $e_{\ell_i} > \hat{e}_{\ell_i}$. Since all equations are trying to converge to P_{\max} with increasing t_ℓ , hence, the change of P_{\max}^ℓ with time i.e., $|P_{\max}^{\ell_{i-1}} - P_{\max}^{\ell_i}|$ will be larger than $|\hat{P}_{\max}^{\ell_{i-1}} - \hat{P}_{\max}^{\ell_i}|$. Let us observe a few time sequences of $P_{\max}^{\ell_i}$ and $\hat{P}_{\max}^{\ell_i}$. If $\hat{P}_{\max}^{\ell_i}$ is closer approximation of P_{\max} , we can expect: $|P_{\max}^{\ell_{i-1}} - P_{\max}^{\ell_i}| < |\hat{P}_{\max}^{\ell_{i-1}} - \hat{P}_{\max}^{\ell_i}|$; for, $i = 2, 3, \dots, m$. Hence by comparing the magnitudes of $|P_{\max}^{\ell_{i-1}} - P_{\max}^{\ell_i}|$ and $|\hat{P}_{\max}^{\ell_{i-1}} - \hat{P}_{\max}^{\ell_i}|$, we can predict which equation approximate the P_{\max} closely.

In our proposed approach, two different equations are trying to approximate two different curves. Equation (7) approximates P-V curve, and (14) approximates P- θ curve. However, the value of maximum (i.e. P_{\max}) is same for the two curves. Hence we can utilize the above observation to compare the prediction accuracy of P_{\max} by an equation.

B. Voltage instability predication algorithm

Let the current time instant be t_ℓ . We assume that we have the measurements of voltage magnitude and angle of all load buses at time instants $\{t_r\}_{r=1}^\ell$. Let at time t_ℓ , the voltage magnitude and angle of a load bus s be $V_{t_\ell}^s$ and $\theta_{t_\ell}^s$ respectively. We can calculate the changes of voltage magnitude, angle and the voltage decline rate [3]

$$\Delta V_{t_\ell}^s = \frac{V_{t_\ell m}^s - V_{t_\ell}^s}{M}; \Delta \theta_{t_\ell}^s = \frac{\theta_{t_\ell m}^s - \theta_{t_\ell}^s}{M};$$

$$\delta(\Delta V_{t_\ell}^s) = \frac{\Delta V_{t_\ell m}^s - \Delta V_{t_\ell}^s}{M}; \quad (18)$$

where $t_\ell > t_{\ell m}$ and $t_\ell - t_{\ell m} = M$ sec. At t_ℓ we run the algorithm in Table I. In Step 2, the value of threshold ξ is set to 0.00015 p.u and $m = 20$ [3]. We set $\epsilon = 0.01$, in Step 5.

C. Tuning parameter τ in (17)

Prior to real-time implementation, we can collect the historical load data of the power system and conduct offline learning to find an appropriate value for τ . Let the historical data shows that the incident of Step2 of the algorithm is satisfied for S number of time instants $\{\kappa_i\}_{i=1}^S$ for different buses. Select a time instant κ_i . The historical data can help us to predict the actual value of P_{\max} and V_{pm} after the incident at κ_i . Now use the value of P_{\max} in (17) instead of \hat{P}_{\max}^ℓ . Tune the value of τ in the range $[10^2, 10^6]$ for which the constraint in (15) is closely satisfied i.e., $\|\frac{\alpha_2(\ell)^2 + 4\alpha_3(\ell)\alpha_1(\ell)}{4\alpha_3(\ell)} - P_{\max}\| < 1^{-3}$. Let the value of τ is indicated by $\hat{\tau}_i$. The procedure is repeated for all times $\{\kappa_i\}_{i=1}^S$. The final value of $\tau = \frac{1}{S} \sum \hat{\tau}_i$.

IV. ADAPTIVE PMU REPORTING OVER WIMAX

Due to the complex dynamic behavior of the power system, the change of voltage of a bus does not remain same over time (see Figure 3(b)). It is quite difficult to predict the future behavior of ΔV . The value of ΔV changes rapidly when the voltage of a load bus reaches closer to the voltage instability. Hence an aggressive PMU reporting rate will be helpful to precisely predict a voltage instability condition.

In a typical synchrophasor network, the first-level data transfer takes place between a group of PMUs and a local PDC (phasor data concentrators) [10]. Since the focus of this paper is local control, we assume that the voltage instability prediction and control process is embedded within the local PDC. Note that such an adaptive PMU reporting scheme is consistent with the recent IEEE C37.118.2 standard for synchrophasor data transfer [10]. The standard allows the PDC to send commands to the PMUs using a command (CMD) frame. The frame has a 2 byte field which can be used to change the synchrophasor reporting states e.g., normal and expedited.

The use of an IEEE 802.16 based WiMAX network for PMU data transfer has been well investigated in [11]. It concludes that the conventional Unsolicited Grant Service (UGS) of WiMAX is the best candidate to transfer the periodic and fixed-size synchrophasor data packets. To enable adaptive reporting, at first the concerned PMU(s) needs to be notified through a CMD message to change its data output. After that, the service flow parameters of the corresponding UGS data connection need to be dynamically modified so that the newly generated bandwidth requirements are met. Such a dynamic negotiation is allowed in the existing WiMAX framework by using the dynamic service change (DSC) procedure [12]. The procedure supports both the SS (Subscriber Station) initiated DSC and the BS (Base Station) initiated DSC. For adaptive reporting, since the upstream PDC is changing the connection properties, the BS needs to initiate the DSC procedure. An important consideration here is that any required bandwidth change needs to be sequenced between the PMU (read SS) and the BS to prevent loss of measurement packets.

V. SIMULATION & RESULTS

The proposed protection scheme has been tested on a modified New England 39-bus power system [13]. According to [13], we need to install PMUs on buses 3, 8, 10, 16, 20, 23, 25, 29 to make the system observable. We consider two types of load parameter setting in (3): i) ZIP load 1: 25% PQ, 75% I in (3); ii) ZIP load 2: 25% PQ, 25% I, and 50% Z. We assume that all loads are changed by the same loading factor k_t and k_t is increasing linearly with time. Performances of the protection scheme are depicted from Figure 3 to Figure 6. We find that when loading factor k_t of all buses changes simultaneously, the voltages in buses 7, 8 and 4 are dropping quickly. Hence those three buses are selected as critical buses. The Figure 3 shows the voltage profile of the three critical buses. As can be seen in Figure 3(b), the change of voltage is not smooth. The decreasing rate of voltage increases quickly when the buses reaches closer to

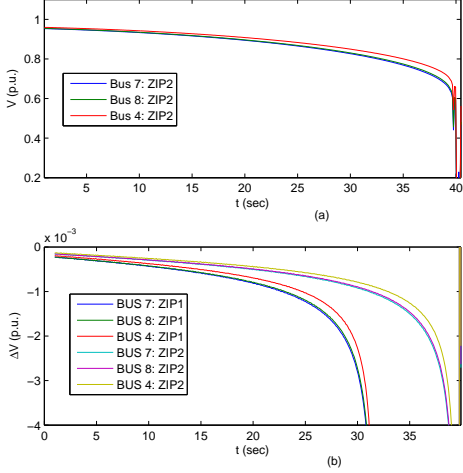


Fig. 3. (a) Voltage profile of three critical load buses. (b) Change of voltage with time of three critical load buses.

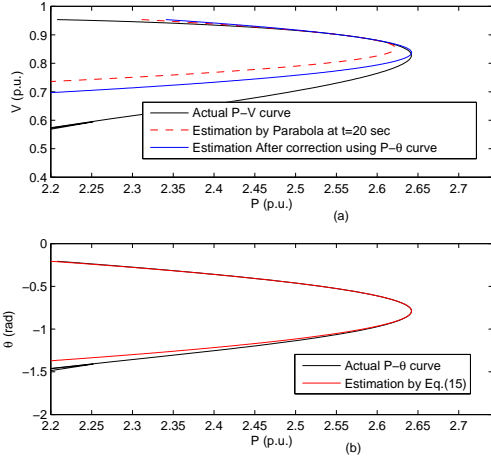


Fig. 4. Estimation of (a) P-V and (b) P- θ characteristic curves of Bus 7 (ZIP 2) by using (7), (10), (14).

the voltage instability. Figure 3(b) also depicted that the time required for reaching voltage instability are different for two different load setting: around 30 sec and 40 sec for ZIP1 and ZIP2 respectively.

We then investigate the estimation accuracy of P-V and P- θ curves by using the techniques proposed in Section III. In Figure 4, we find that at $t = 20$ sec the P- θ curve estimation by using (14) is more accurate than the P-V curve estimation by using (7). Hence we utilize the optimization in (15) to predict P_{\max} . Figure 4 (a) shows that the estimation of P_{\max} after correction is more accurate.

In normal operation, the PMU sends a set of previous time samples of the bus voltage V_t to the processing center at every 2 sec. In the adaptive PMU reporting scheme, the PMU reporting interval changed to 20 ms (Step3 of the algorithm) when the condition of Step2 of the algorithm in Table-I is satisfied at 10th sec (see Figure 3). We investigate the performance of both adaptive and non-adaptive reporting

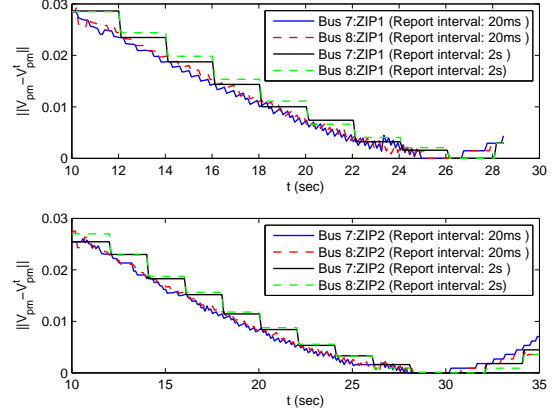


Fig. 5. Evolution of estimation error of V_{pm} (voltage corresponding to P_{\max}) for different loading conditions. See STEP 11 of the algorithm.

scheme. In non-adaptive scheme, Step3 of the algorithm is ignored, i.e., the PMU reporting interval remains fixed to 2 sec. At every reporting, we estimate V_{pm} and V_C . Figure 5 shows the evolution of estimation accuracy of V_{pm} with time for different types of loading on Bus 7 and Bus 8. As can be seen in Figure 5, the estimation error is decreasing with increasing t . In adaptive case, the estimation error is 0.0228 p.u. at $t = 10$ sec and the error is 0.008p.u. at $t = 20$ sec for Bus 7 (ZIP 2). The similar types of results are obtained for ZIP 1 type loading. The estimation error is updating smoothly in adapting scheme compared to non-adaptive scheme. In adaptive scheme, the estimation error of the V_{pm} of Bus 7 (ZIP1) are 0.02348, 0.02095, 0.0198, 0.0187 p.u. at 12, 13, 13.5 and 14th sec respectively. In fact, the estimation is updated 100 times between 12 – 14 sec. On the other hand the estimation error, are 0.02348, 0.02348, 0.02348, 0.0187 p.u. at 12, 13, 13.5 and 14th sec respectively for non-adaptive case. The estimation error did not update in the interval between 12 – 14 sec. Hence, adaptive scheme allows us to observation the system status closely. At every reporting, we also estimate the time t_{pm}, t_* required to reach V_{pm} and V_C respectively. Figure 6 shows that the perdition accuracy of t_* is also increasing with t . For adaptive case, at $t = 11$ sec, we see that the voltage of Bus 7 will be unstable after $t_* = 19.5$ sec, i.e. we have 19.5 sec to take control action. We also try to estimate t_* at $t = 11$ sec by our algorithm (Step12, Step13, Step14). The estimation of t_* is 17 sec. At $t = 15$ sec, the actual t_* and computed t_* are almost same. Hence, we get sufficient time to take proper control action. We also found that the frequency of updating of t_{pm}, t_* for non-adaptive case are slower increasing the probability of producing false alarm.

To examine the effect of the proposed synchrophasor reporting scheme on the WiMAX network, we develop a single cell simulation model using the OPNET modeler 16.0. For the sake of simplicity, an ideal propagation channel was considered for the simulation trial. The key WiMAX simulation parameters are listed in Table II. Here, we assume that a single WiMAX cell is sufficient to cover the service area of the New England 39-bus test system considered for this study. The number of

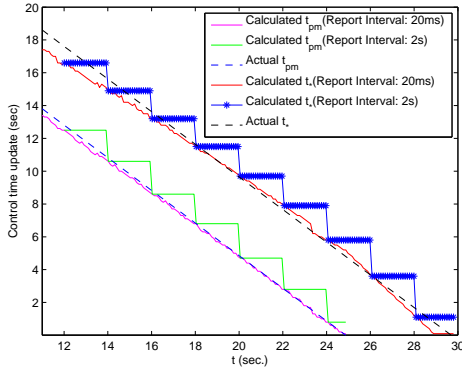


Fig. 6. Estimation of time required to reach voltage instability (see Step12, step13, step14 of the algorithm) for Bus 7 with ZIP load 1.

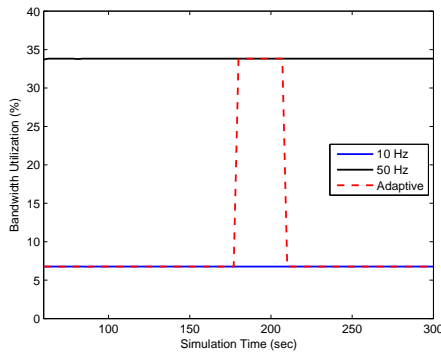


Fig. 7. Bandwidth Utilization of the WiMAX Uplink Subframe under the adaptive and the non-adaptive synchrophasor reporting schemes.

PMUs considered for this simulation is 8. The mean PMU payload size is assumed to be of 100 bytes.

While at a given instance only a particular bus or a set of buses may be in the risk of voltage instability, considering the worst case scenario we assume that the PDC increases the reporting rates for all 8 PMUs simultaneously from 10 Hz to 50 Hz during the 3rd minute of an observation period of 5 minutes. The expedited reporting rate exists for 30 seconds after which the system becomes stable again. Fig.7 shows the bandwidth utilization of the WiMAX uplink subframe under adaptive and non-adaptive reporting schemes. The results show that the proposed scheme consumes bandwidth more efficiently than the non-adaptive scheme. To sum up, while the higher reporting rates need more bandwidth and lower reporting rates compromise the performance of the prediction algorithm, an adaptive reporting rate provides the optimum solution by increasing its bandwidth needs only when it is required.

VI. CONCLUSION

In this paper, we explore a framework of the power system voltage instability prediction problem by using the system P- θ and P-V characteristics. An adaptive PMU reporting scheme is also introduced which can utilize the communications media more efficiently. The proposed approach does not require continuous tracking of the Thevenin equivalent of the system and

TABLE II
WiMAX SIMULATION PARAMETERS

Parameters	Values
Physical Layer	OFDMA, TDD
Operating Frequency	2.3 GHz
System Bandwidth	5 MHz (FFT 512)
Modulation and Coding	QPSK, $\frac{1}{2}$ Rate
Frame Duration	5 ms
UL:DL Ratio	1:1
Cell Radius	4 km
Path-loss Model	Free Space

it is not very sensitive to the selection of different thresholds, unlike [3]. Hence, the proposed scheme can overcome some of the limitations of a localized control system.

While WiMAX is one of many prospective communications solutions for the proposed protection scheme, the key applications requirement is to meet the end-to-end latency of the synchrophasor data packets at all reporting rates. This can be done by providing reservation-based bandwidth grants (such as the UGS service in WiMAX) at each measurement cycle. Moreover, the change of reporting rates should be carefully coordinated using a handshaking procedure so that no packets are lost during the changeover time, especially from low to high reporting rates as the system is moving towards the voltage instability point.

REFERENCES

- [1] "Use of synchrophasor measurements in protective relaying," *IEEE Power and Energy Society*, Dec. 2011.
- [2] B. Milosevic and M. Begovic, "Voltage-stability protection and control using a wide-area network of phasor measurements," *Power Systems, IEEE Transactions on*, vol. 18, no. 1, pp. 121–127, Feb. 2003.
- [3] R. Sodhi, S. Srivastava, and S. Singh, "A simple scheme for wide area detection of impending voltage instability," *Smart Grid, IEEE Transactions on*, vol. 3, no. 2, pp. 818–827, June, 2012.
- [4] Y. Gong, N. Schulz, and A. Guzman, "Synchrophasor-based real-time voltage stability index," in *Power Systems Conference and Exposition, 2006. PSCE '06. 2006 IEEE PES*, 29 2006–Nov. 1, pp. 1029–1036.
- [5] S. Corsi and G. Taranto, "A real-time voltage instability identification algorithm based on local phasor measurements," *Power Systems, IEEE Transactions on*, vol. 23, no. 3, pp. 1271–1279, Aug. 2008.
- [6] K. Seethalekshmi, S. Singh, and S. Srivastava, "A synchrophasor assisted frequency and voltage stability based load shedding scheme for self-healing of power system," *Smart Grid, IEEE Transactions on*, vol. 2, no. 2, pp. 221–230, June, 2011.
- [7] "Standard load models for power flow and dynamic performance simulation," *Power Systems, IEEE Transactions on*, vol. 10, no. 3, pp. 1302–1313, Aug. 1995.
- [8] H. Bai, P. Zhang, and V. Ajjarapu, "A novel parameter identification approach via hybrid learning for aggregate load modeling," *Power Systems, IEEE Transactions on*, vol. 24, no. 3, pp. 1145–1154, Aug. 2009.
- [9] N. Niglye, F. Peritore, R. Soper, C. Anderson, R. Moxley, and A. Guzman, "Considerations for the application of synchrophasors to predict voltage instability," in *Power Systems Conference: Advanced Metering, Protection, Control, Communication, and Distributed Resources, 2006. PS '06*, March, pp. 169–172.
- [10] I. . 2011, "IEEE standard for synchrophasors data transfer for power systems," Dec. 2011.
- [11] R. H. Khan and J. Y. Khan, "Wide area PMU communication over a WiMAX network in the smart grid," in *IEEE Smart Grid Comms.*, 2012, pp. 1–6.
- [12] I. 802.16-2009, "IEEE standard for local and metropolitan area networks Part 16: Air interface for fixed and mobile broadband wireless access systems," May 2009.
- [13] S. Chakrabarti and E. Kyriakides, "Optimal placement of phasor measurement units for power system observability," *Power Systems, IEEE Transactions on*, vol. 23, no. 3, pp. 1433–1440, Aug. 2008.